Schizophrenia Research 213 (2019) 96–106

Contents lists available at ScienceDirect

Schizophrenia Research

journal homepage: www.elsevier.com/locate/schres

A developmental redox dysregulation leads to spatio-temporal deficit of parvalbumin neuron circuitry in a schizophrenia mouse model

Jan-Harry Cabungcal [a], Pascal Steullet [a], Rudolf Kraftsik [b], Michel Cuenod [a], Kim Q. Do [a,*]

[a] Center for Psychiatric Neuroscience, Department of Psychiatry, Lausanne University Hospital-CHUV, Prilly-Lausanne, Switzerland
[b] Department of Fundamental Neurosciences, University of Lausanne, Lausanne, Switzerland

ARTICLE INFO

Article history:
Received 6 December 2018
Received in revised form 19 February 2019
Accepted 22 February 2019
Available online 8 March 2019

Keywords:
Functional connectivity
Neurodevelopment
Oxidative stress
Parvalbumin
Perineuronal nets
Schizophrenia

ABSTRACT

The fast-spiking parvalbumin (PV) interneurons play a critical role in neural circuit activity and dysfunction of these cells has been implicated in the cognitive deficits typically observed in schizophrenia patients. Due to the high metabolic demands of PV neurons, they are particularly susceptible to oxidative stress. Given the extant literature exploring the pathological effects of oxidative stress on PV cells in cortical regions linked to schizophrenia, we decided to investigate whether PV neurons in other select brain regions, including sub-cortical structures, may be differentially affected by redox dysregulation induced oxidative stress during neurodevelopment in mice with a genetically compromised glutathione synthesis (*Gclm* KO mice). Our analyses revealed a spatio-temporal sequence of PV cell deficit in *Gclm* KO mice, beginning with the thalamic reticular nucleus at postnatal day (P) 20 followed by a PV neuronal deficit in the amygdala at P40, then in the lateral globus pallidus and the ventral hippocampus Cornu Ammonis 3 region at P90 and finally the anterior cingulate cortex at P180. We suggest that PV neurons in different brain regions are developmentally susceptible to oxidative stress and that anomalies in the neurodevelopmental calendar of metabolic regulation can interfere with neural circuit maturation and functional connectivity contributing to the emergence of developmental psychopathology.

1. Introduction

Cortical inhibitory neurons that express parvalbumin (PV) are known to modulate information flow in neural circuits essential for cognitive processing (Lewis et al., 2012). These neurons are widely distributed in the brain (Ohshima et al., 1991), where they selectively target the soma and the axon initial segments of pyramidal neurons and contribute to the generation of gamma oscillatory activity (Sohal et al., 2009). In particular, deficits of PV neurons, especially in the prefrontal cortex and hippocampus, are among the most replicated findings in postmortem brain samples from individuals with schizophrenia (Beasley and Reynolds, 1997; Benes et al., 1991; Hashimoto et al., 2003; Zhang and Reynolds, 2002). These disturbances in PV neurons are believed to affect cognitive operations that require gamma oscillations, including attention and working memory, both of which are affected in schizophrenia (Gonzalez-Burgos et al., 2015; Uhlhaas and Singer, 2015).

Due to their fast and high frequency discharges, PV neurons exhibit elevated metabolism, increased mitochondrial activity and a high production rate of reactive oxygen species (Kann et al., 2014). As a result, PV neurons are particularly susceptible to oxidative stress (Kann, 2016). In this regard, a recent spate of studies has implicated oxidative stress in the pathophysiology of schizophrenia (Do et al., 2009; Steullet et al., 2016), with some of the evidence pinpointing neurobiological anomalies such as abnormal myelination (Monin et al., 2015) and a functional alteration in PV neurons (Behrens et al., 2007; Cabungcal et al., 2006, 2013a, 2013b; Giavanoli et al., 2015; Lodge et al., 2009; Meechan et al., 2015; Steullet et al., 2010, 2017a).

Indeed, research from our laboratory has demonstrated alterations of PV-containing neurons, manifested by a decreased immunoreactivity of PV and perineuronal nets (PNNs, extracellular matrix structures that coat PV neurons and provide protection against oxidative stress), in both the anterior cingulate cortex (ACC) and ventral hippocampus (VH) of transgenic mice carrying a germline deletion of the modulatory subunit (GCLM) of the glutamate-cysteine ligase holoenzyme (Cabungcal et al., 2013a, 2013b; Kulak et al., 2013; Steullet et al., 2010), the rate-limiting enzyme in the glutathione (GSH) biosynthesis pathway. Notably, transgenic *Gclm* knock-out mice exhibit a deficit in GSH synthesis, leading to a 60–70% reduction of brain GSH levels that results in an increased susceptibility to oxidative stress (Steullet et al., 2010). In a more recent study animal models carrying genetic and/or environmental

* Corresponding author at: Centre de Neurosciences Psychiatriques, Département de Psychiatrie, Route de Cery, CH-1008 Prilly-Lausanne, Switzerland.
E-mail address: Kim.Do@chuv.ch (K.Q. Do).

https://doi.org/10.1016/j.schres.2019.02.017

risks relevant to schizophrenia were found to exhibit PV neuron deficits that were accompanied by oxidative stress in the ACC (Steullet et al., 2017a, 2017b). This study indicates that a diversity of pathological mechanisms (i.e. redox dysregulation, NMDA-R hypofunction) can converge to oxidative stress induced PV neuron impairments. Noteworthy, neuroimmune dysregulation during neurodevelopment can also generate and maintain oxidative stress in a feed-forward fashion, leading to a vicious and enduring cycle that has detrimental effects on PV neurons in the ACC (Dwir et al., 2017). Other evidence has shown oxidative stress to affect PV neuron integrity in hippocampal structures such as the dentate gyrus and Cornu Ammonis (CA) 3 region (Kann et al., 2011; Steullet et al., 2010). These cellular deficits were associated with alterations of beta/gamma oscillations (Kann et al., 2011; Steullet et al., 2010). Notably, gamma oscillatory activity has consistently been found to be disturbed in schizophrenia (Gonzalez-Burgos et al., 2015; Uhlhaas and Singer, 2015).

Despite the preponderance of data indicating the effects of oxidative stress-driven PV impairment in cortical structures such as the ACC and VH, little is known of the sequelae of oxidative stress in PV neurons situated in sub-cortical structures that might be affected in schizophrenia neuropathology. This research gap served as the impetus for the present study, which aimed to answer two specific questions: (1) if PV-containing neurons situated in sub-cortical regions of the brain are similarly affected by oxidative stress and (2) whether a developmental sequence may exist in their susceptibility to oxidative stress induced impairments. To address these points, we followed the developmental sequence of PV cell impairments, in *Gclm* KO mice, in several brain regions known to be involved in the schizophrenia physiopathology, i.e., the thalamic reticular nucleus, amygdala, lateral globus pallidus, ventral hippocampus and anterior cingulate cortex. Elucidating the spatio-temporal profile of neuropathology which impacts specific neuronal subsets during brain development is key to understanding neurodevelopmental disorders, and is expected to yield information on how neural circuit disturbances could underlie symptomatology in psychiatric disorders characterized by altered cognition such as schizophrenia.

2. Materials and methods

2.1. General methodology

Using a confocal microscope, three to four scanned stack images (per animal) were collected from the thalamic reticular nucleus (TRN), amygdala (AMY), lateral globus pallidum (LGP), CA3 of ventral hippocampus (VH) and anterior cingulate cortex (ACC) of male *Gclm* KO (n = 25) and WT (n = 25) mice, to analyze the expression of: 1) oxidative stress, 2) PV positive cells and 3) perineuronal nets (PNNs) at postnatal days (P) 20, 40, 90, 120 and 180 (5 mice per genotype and age).

2.2. Animal model

Glutamate cysteine ligase modifier subunit knock-out (*Gclm* KO) mice (B6.129-Gclmtm1Tdal) initially provided by T. Dalton (University of Cincinnati) were backcrossed with C57BL/6J mice over >10 generations. Mice were housed under a 12-h light-dark cycle in groups of 3–5 individuals per cage. All breeding mice were obtained from heterozygotes (HZ x HZ). Experimental *Gclm* KO mice were from breeding individuals (males KO x females HZ), and control *Gclm* WT mice were from breeding individuals (WT x WT). Experiments were performed on males (5 per genotype) and were approved by the Cantonal Veterinary Office.

2.3. Perfusion and preparation

Mice were anesthetized and perfused (5 mice genotype and age; n = 50), and their brains fixed in 4% paraformaldehyde (Cabungcal et al., 2006). Coronal frozen sections (50 μm) were prepared and stored in ethylene glycol at −20 °C until immunohistochemistry procedure.

2.4. Immunofluorescence, confocal imaging and image analysis

For each mouse (n = 50), brain sections (3–4 per sections per mice and region) containing the regions of interest (i.e., TRN, AMY, LGP, CA3 of VH, ACC) were first incubated with PBS + Triton 0.3% + sodium azide (1 g/L) containing 2–3% normal horse serum, then placed for 48 h in a solution with a mouse monoclonal anti-8-oxo-dG (1:400; AMS Biotechnology, Biogio-Lugano, Switzerland) and a rabbit polyclonal anti-parvalbumin (1:2500; Swant Inc., Marly-Fribourg, Switzerland) primary antibody together with the biotin-conjugated lectin *Wisteria floribunda* Agglutinin (WFA, 1:2000; Sigma, Switzerland). Sections were then washed, incubated with fluorescent secondary antibody conjugates: goat anti-mouse (1:300; A488; Life Technologies, USA), goat anti-rabbit IgG (1:300; CY3; Chemicon International, USA) and streptavidin 405 conjugate (1:300; A405; Millipore Corporation, USA), to visualize 8-oxo-dG, PV and WFA labeling.

All brain sections were visualized and processed with a Zeiss confocal microscope equipped with x10, x40 and x63 Plan-NEOFLUAR objectives. All peripherals were controlled with LSM 710 Quasar software (Carl Zeiss AG, Switzerland). Z stacks of 12 images (with a 2.13 μm interval) were scanned (1024 × 1024 pixels) with ×10, ×20 and ×63 objectives for analysis and qualitative investigation with IMARIS 7.3 software (Bitplane AG, Switzerland). Three to four sections consisting of fully intact and undamaged region of interests (ROIs) (e.g., from TRN: at ~ Bregma: −0.82 to −0.94 mm, and Interaural: 2.98 to 2.68 mm, from AMY and LGP: at Bregma: −1.22 to −1.34 mm, and Interaural: 2.58 to 2.46 mm, and from ACC: Bregma: −1.10 to 0.62 mm, and Interaural: 4.90 to 4.42 mm) was used to do cell count and intensity quantification. The ROI for AMY included the dorsolateral amydaloid nucleus and anterior basolateral amygdala nucleus. The ROIs were defined and marked throughout the inner 8 images of *Z*-stacks to isolate regional sub-volumes of the investigated structures, in which 8-oxo-dG labeling, the number of PV cells and WFA/PNNs were quantified.

To quantify the overall 8-oxo-dG fluorescent / staining intensity in the ROI, we used the Coloc module of the IMARIS software to calculate the proportion of all 8-oxo-dG immunolabeled voxels and the mean labeling intensity. To analyze the number of PV cells and PV cells surrounded by WFA/PNN (WFA/PV cells), we used the spots module to assign spot markings on the profile-labeled voxels that fall within a given size. Briefly, the channels for PV and WFA immunolabeling were chosen, and the profile size criterion (10 and 8 μm, respectively) was defined to quantify stained profiles above these given sizes. The procedure was visually monitored/verified before proceeding. Spots generated for PV cells that contacted / overlapped with spots generated for WFA, were considered as WFA (PNN) PV cells. We also assessed PNNs by quantifying the overall intensity of WFA immunolabeling (in arbitrary unit).

2.5. Statistical analyses

A two-way multivariate analysis of variance (ANOVA) with PV+ cell density, WFA+ PV cells and 8-oxo-dG intensity as dependent variables, and genotype and age as fixed effects were performed for each brain region followed by univariate ANOVA analysis. Post-hoc Dunnett's *t*-tests were performed to compare the mean number of

PV cells, WFA (PNN)/ PV cells, and the overall 8-oxo-dG and WFA-labeling between the groups (WT vs. KO). All statistics were performed using (JMP 12, SAS Institute Inc., Cary NC, USA) statistical software. All statistics were two-tailed with a preset alpha level for significance of $p < 0.05$.

3. Results

Data were collected from five pre-specified brain regions (thalamic reticular nucleus, amygdala, lateral globus pallidum, CA3 of ventral hippocampus, anterior cingulate cortex, based upon the presence of PV expression and their clinical relevance to schizophrenia, at five distinct developmental ages (postnatal day (P) 20, 40, 90, 120 and 180). Three way multivariate analysis of variance with PV+ cell density, PV cells ensheathed by WFA-labeled PNNs and 8-oxo-dG intensity as dependent variables taking ROI, genotype and age as fixed effects showed a significant effect for region, age and genotype ($p < 0.0001$).

3.1. Thalamic reticular nucleus

The TRN is comprised of a narrow sheath of GABAergic neurons, especially those expressing PV (Jones and Hendry, 1989), that are involved in "gating" cortico-thalamic communications (Crick, 1984; Halassa and Acsády, 2016). This distinct thalamic nucleus plays a key role in modulating various cognitive functions such as attention and sleep that are commonly affected in individuals with schizophrenia (Ferrarelli and Tononi, 2011; Young and Wimmer, 2017). The multivariate ANOVA shows a significant effect for age ($F_{(6,64)} = 12.7$, $p < 0.001$) and genotype ($F_{(3,22)} = 37.2$, $p < 0.001$).

Representative immunofluorescence images for expression of the DNA oxidation product 8-oxo-dG, a marker of oxidative stress, PV and WFA, in the TRN from WT and *Gclm* KO animals at P20 are illustrated in Fig. 1A. We observed an oxidative stress related deficit in PV cells in the TRN that emerged at P20. Consistent with recent published research from our group (Steullet et al., 2017a, 2017b), we found a significant and gradual increase in 8-oxo-dG expression levels from the juvenile development phase (P20) through to adulthood in the *Gclm* KO mice compared to their WT counterparts (Fig. 1B). Indeed, an ANOVA revealed a significant overall effect of age on 8-oxo-dG expression intensity ($F_{(2,24)} = 9.7$, $p = 0.001$) and a significant main effect of genotype ($F_{(1,24)} = 39.1$, $p < 0.0001$). Subsequent analysis of PV neuron density in TRN revealed a significant overall effect of age (Fig. 1C: $F_{(2,24)} = 5.8$, $p = 0.009$) and a significant

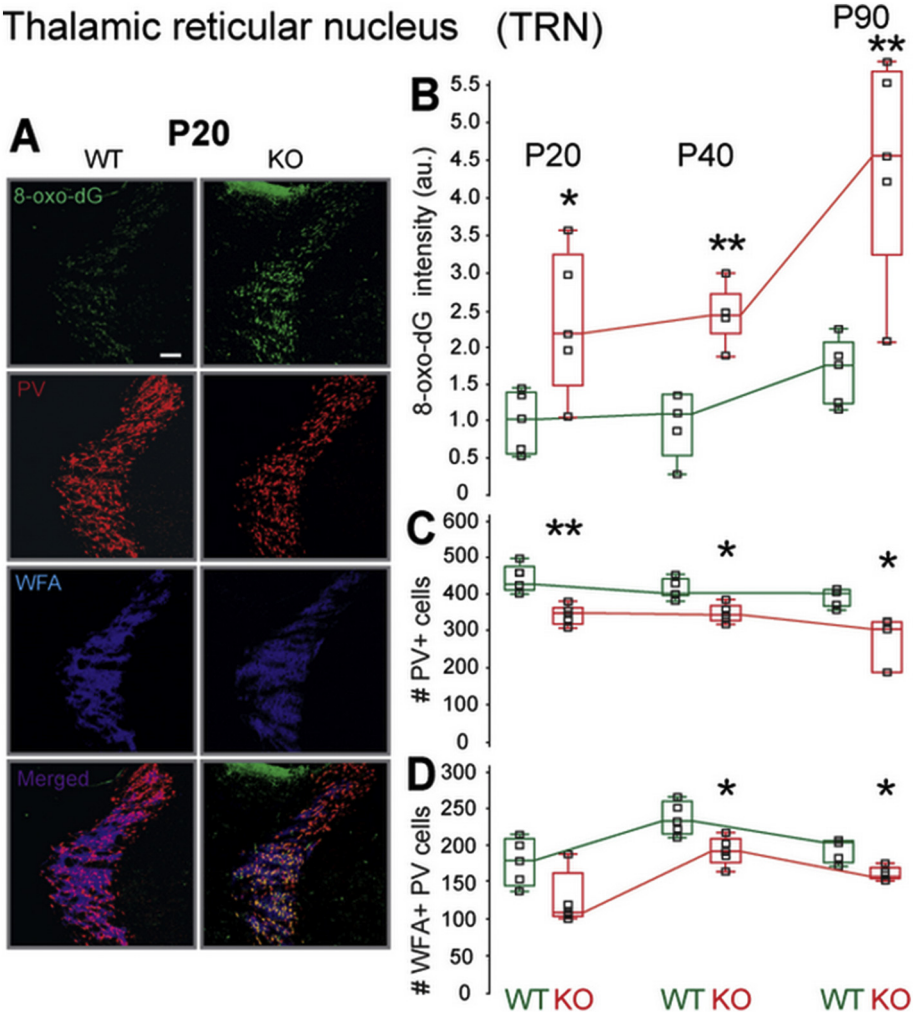

Fig. 1. A developmental redox dysregulation led to early increase and long lasting oxidative stress, and PV+ cells and WFA+ (PNN) PV cell deficit in the TRN of *Gclm* KO mice. (A) Micrographs show immunofluorescent labeling for 8-oxo-dG (green), PV+ cells (red) and WFA+ PNN (blue) in the TRN of P20 (Juvenile) *Gclm* KO mice. (B) Increased 8-oxo-dG immunolabeling intensity (arbitrary unit, a.u.) in KO was already present at P20 (juvenile), maintained at P40 (adolescent) and even higher at P90 (adulthood). (C) The number of PV+ cells decreased in TRN KO, across all ages, as compared to WT mice. (D) WFA+ (PNN) PV cells in the TRN of KO mice began to be significantly reduced at P40 (adolescent) and maintained at P90 (adulthood), when compared to WT mice. For each group, $n = 5$. Scale: 80 μm. Each bar depicts where the 25 and 75% of data points lie. The horizontal line inside the bar and the boxes depicts the median and average data point (from 3 to 4 samples per animal), respectively. *$p = 0.05$; **$p = 0.001$ (pair-wise Dunnett's tests). KO, knock out; PNN, perineuronal net; PV, parvalbumin; TRN, thalamic reticular nucleus; WFA, *Wisteria floribunda* agglutinin; WT, wild type.

main effect of genotype ($F_{(1,24)} = 36.0$, $p < 0.0001$). Post-hoc comparisons showed a significant decrease of PV cells already in P20 *Gclm* KO mice as compared with age-matched WT (WT ($M = 442.9 \pm 36.9$) vs. *Gclm KO* ($M = 340.3 \pm 24.3$, $t_{(6.9)} = 5.2$, $p = 0.002$). An analysis of the number of PV cells enwrapped by PNNs revealed a significant main effect of age (Fig. 1D: $F_{(2,24)} = 17.1$, $p < 0.0001$) and genotype ($F_{(1,24)} = 18.8$, $p = 0.0002$). Post-hoc comparisons revealed a significant reduction in the number of PV cells surrounded by a PNN in *Gclm* KO mice in the P40 [WT ($M = 411.2 \pm 14.7$) vs. *Gclm KO* ($M = 345.2 \pm 25.9$)] and the P90 [WT ($M = 388.9 \pm 25.2$) vs. *Gclm KO* ($M = 261.7 \pm 80.8$)] cohort relative to WT controls.

3.2. Amygdala

A constellation of evidence from preclinical and clinical studies has linked neural circuit deficits associated with the amygdala to schizophrenia and developmental psychopathology (Benes and Berretta, 2001). The multivariate ANOVA shows a significant effect for age ($F_{(6,44)} = 4.7$, $p < 0.001$) and genotype ($F_{(3,22)} = 25.5$, $p < 0.001$). Immunofluorescent imaging of 8-oxo-dG, PV and WFA in the AMY from WT and *Gclm* KO animals at P40 are illustrated in Fig. 2A. We found the effects of oxidative stress to start affecting PV-containing neurons in the AMY at P40. An ANOVA on 8-oxo-dG labeling within AMY identified a significant overall effect of age (Fig. 2B: $F_{(2,24)} = 6.9$, $p = 0.004$). Post-hoc comparisons revealed a significant increase in 8-oxo-dG starting at P40 in the AMY of *Gclm* KO mice as compared with age-matched WT ($t_{(6.3)} = 6.8$, $p = 0.009$). Analysis of PV neuronal density within AMY revealed a significant genotype (Fig. 2C: $F_{(1,24)} = 20.3$, $p = 0.0001$). Post-hoc comparisons showed a significant decrease of PV cells starting at P40 *Gclm* KO mice as compared with age-matched WT ($t_{(8.0)} = 2.3$, $p = 0.04$). An ANOVA of the number of PV cells coated with a PNN similarly revealed a significant effect of age ($F_{(2,24)} = 185.6$, $p < 0.0001$) and genotype ($F_{(2,24)} = 14.1$, $p = 0.001$, Fig. 2D). Post-hoc comparisons revealed a significant reduction in the number of PV cells surrounded by a PNN in *Gclm* KO mice in the P40 [WT ($M = 28.4 \pm 4.0$) vs. *Gclm KO* ($M = 22.1 \pm 3.3$)] and the P90 [WT ($M = 18.0 \pm 1.5$) vs. *Gclm KO* ($M = 15 \pm 1.5$)] cohort relative to WT controls.

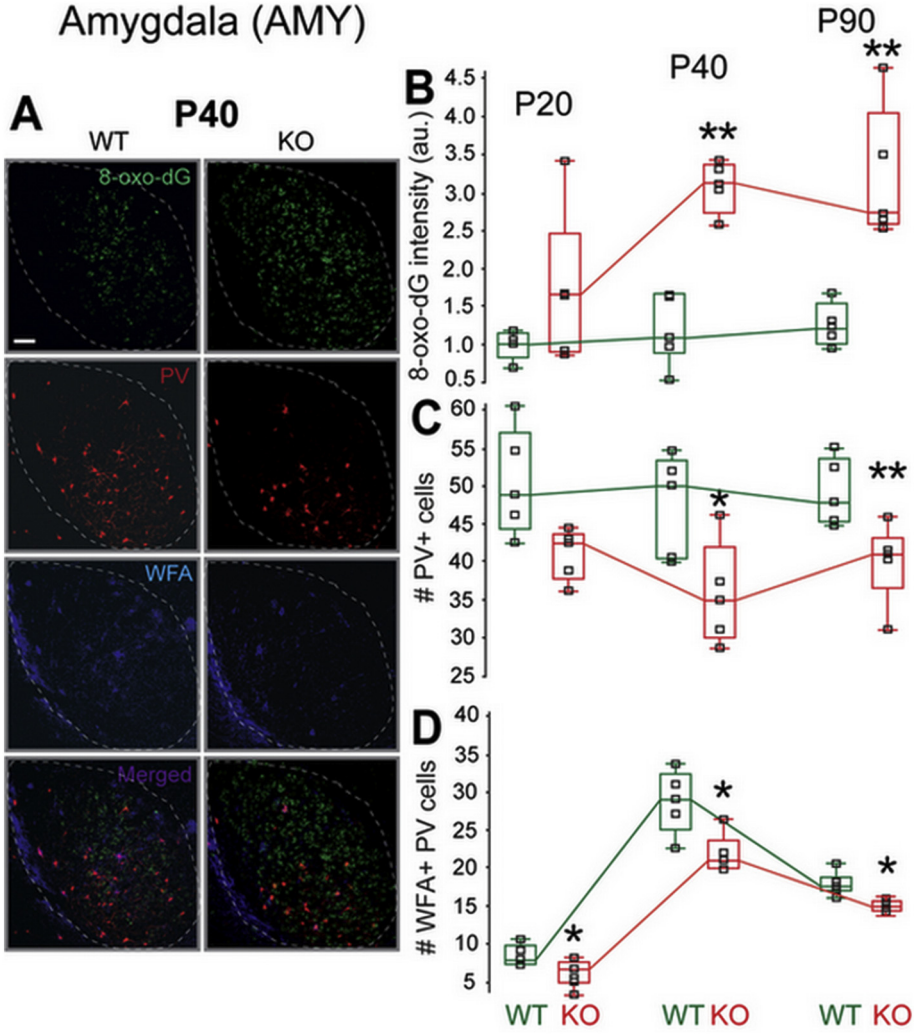

Fig. 2. A developmental redox dysregulation led to adolescent oxidative stress and adolescent PV+ cells and WFA+ PV deficit in the Amygdala (AMY) of *Gclm* KO that persist until adulthood. (A) Micrographs show immunofluorescent labeling for 8-oxo-dG (green), PV+ cells (red) and WFA+ PNN (blue) in the AMY of P40 (adolescent) *Gclm* KO mice. (B) The 8-oxo-dG labeling intensity (arbitrary unit, a.u.) in KO increased at P40 (adolescent), and persists until P90 (adulthood). (C) The number of PV+ cells decreased in AMY of KO, at P40 (adolescent) and P90 (adulthood), when compared to WT mice. (D) The number of WFA+ (PNN) PV cells in KO mice (compared to WT) was significantly reduced across all ages: at P20 (juvenile), P40 (adolescent) and P90 (adulthood). For each group, n = 5. Scale: 80 μm. Each bar depicts where the 25 and 75% of data points lie. *$p = 0.05$; **$p = 0.01$ (pair-wise Dunnett's tests). KO, knock out; PNN, perineuronal net; PV, parvalbumin; AMY, Amygdala (delineated as shown by white dotted line in A); WFA, *Wisteria floribunda* agglutinin; WT, wild type.

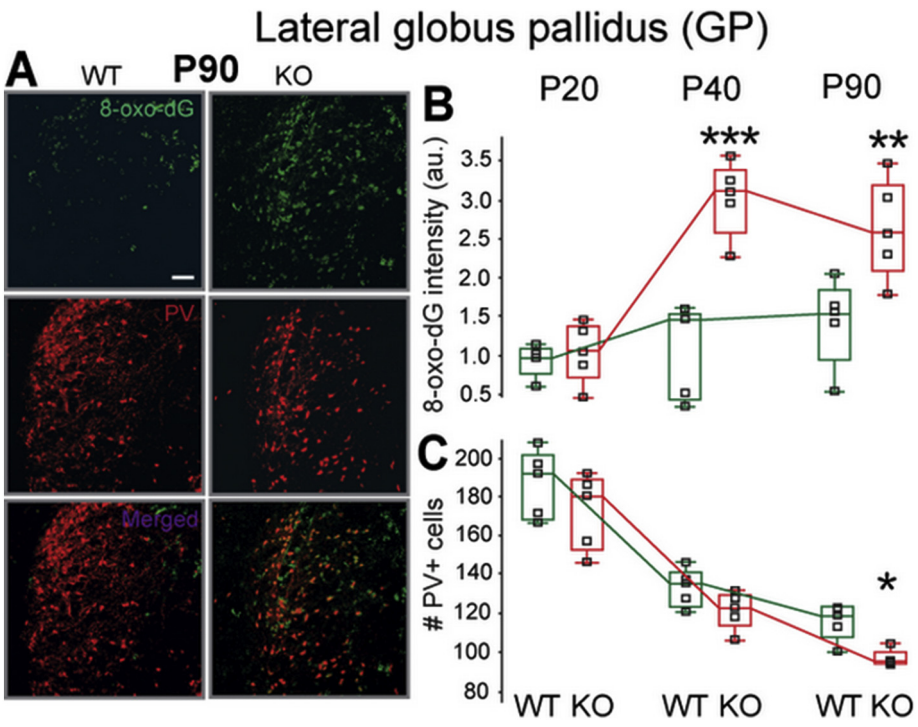

Fig. 3. Persistent redox dysregulation led to adolescent oxidative stress and adult PV+ cells deficit in the lateral globus pallidus (LGP) of *Gclm* KO compared to WT mice. (A) Micrographs show immunofluorescent labeling for 8-oxo-dG (green) and PV+ cells (red) in the LGP of P40 (adolescent) *Gclm* KO mice. (B) 8-oxo-dG labeling intensity (arbitrary unit, a.u.) in KO (red) was significantly increased in both P40 (adolescent) and P90 (adulthood). (C) The number of PV+ cells decreased in LGP of KO only in P90 (adulthood). Since WFA labeling in LGP was different from the observed WFA+ PNNs in TRN, AMY, VH and ACC, this was not included in the analysis. For each group, n = 5. Scale: 80 μm. Each bar depicts where the 25 and 75% of data points lie. $*p = 0.05$; $**p = 0.01$, $***p < 0.001$ (pair-wise Dunnett's tests). KO, knock out; PV, parvalbumin; WT, wild type.

3.3. Lateral globus pallidus

The lateral globus pallidus or globus pallidus externus is predominantly made up of PV expressing neurons (Saunders et al., 2016). It forms part of the basal ganglia circuit and has been linked to the etiology of schizophrenia (Graybiel, 1997; Robbins, 1990). Immunofluorescence staining of 8-oxo-dG and PV in the LGP from WT and *Gclm KO* mice at P90 are illustrated in Fig. 3A. Since WFA labeling in LGP was different from the observed WFA-labeled PNNs in TRN, AMY, VH and ACC, this was not included in the analysis. We detected initial impairments of PV-containing neurons in the LGP at P90. Within the LGP, PV cell density and 8-oxo-dG labeling density varied significantly with age (PV cell density: $F_{(2,24)} = 93.0$ $p < 0.0001$ and for 8-oxo-dG labeling, $F_{(2,24)} = 13.1$, $p = 0.0001$). Both PV cell density and 8-oxo-dG labeling intensity also varied significantly with genotype (PV cell density: $F_{(2,24)} = 13.3$, $p = 0.001$ and for 8-oxo-dG labeling, $F_{(2,24)} = 31.7$, $p < 0.0001$). However, a significant interaction between genotype and age was only observed with 8-oxo-dG intensity ($F_{(2,24)} = 8.0$, $p = 0.002$). Compared with WT animals, labeling for 8-oxo-dG was significantly higher in *Gclm* KO mice at P40 [WT ($M = 1.2 \pm 0.5$) vs. *Gclm KO* ($M = 3.1 \pm 0.5$), ($t_{(7.5)} = 5.2$, $p = 0.001$), and P90 [WT ($M = 1.45 \pm 0.5$) vs. *Gclm KO* ($M = 2.6 \pm 0.7$), $t_{(7.5)} = 3.1$, $p = 0.01$]. However, post-hoc comparisons revealed a significant reduction in PV cell density in *Gclm* KO mice only at P90 [WT ($M = 122.2 \pm 5.5$) vs. *Gclm KO* ($M = 95.2 \pm 9.5$), $t_{(7.5)} = 4.1$, $p = 0.004$].

3.4. Ventral hippocampus

A loss of CA3 GABAergic interneuron phenotype has been reported in patients with schizophrenia and bipolar disorder (Zhang and Reynolds, 2002; Benes et al., 2007). As for the LGP, we found that the impairments of PV-containing neurons within the CA3 region of VH from *Gclm KO* mice emerged at P90, a result consistent with a previous report (Steullet et al., 2010). Immunofluorescence staining of 8-oxo-dG, PV and WFA in the LGP from WT and *Gclm KO* mice at P90 are illustrated in Fig. 4A. ANOVA of 8-oxo-dG labeling in the VH found a significant age effect (Fig. 4B: $F_{(2,24)} = 4.7$, $p = 0.02$) and genotype effect ($F_{(1,24)} = 15.3$, $p = 0.0007$) Post-hoc comparisons revealed a significant elevation in 8-oxo-dG labeling intensity in *Gclm* KO mice at P90 [WT ($M = 0.56 \pm 0.23$) vs. *Gclm KO* ($M = 1.0 \pm 0.12$), $t_{(6.3)} = 3.9$, $p = 0.007$]. Other analysis conducted on PV cell density within the VH revealed a significant age effect (Fig. 4C: $F_{(2,24)} = 24.5$, $p = 0.0001$) and a significant interaction between genotype and age (Fig. 4C: $F_{(2,24)} = 7.6$, $p = 0.003$). A significant decrease in PV neuronal number in *Gclm* KO mice at P90 [WT ($M = 11.7 \pm 1.5$) vs. *Gclm KO* ($M = 7.7 \pm 1.0$), $t_{(6.9)} = 5.0$, $p = 0.002$] was observed. Lastly, ANOVA performed on the number of PV cells co-expressing WFA revealed significant effect of genotype (Fig. 4D: $F_{(1,24)} = 12.3$, $p = 0.002$) but no interaction between genotype and age ($F_{(2,24)} = 1.4$, $p = 0.26$). Post-hoc comparisons revealed a significant reduction in the number of PV cells surrounded by a PNN in *Gclm* KO mice in the P90 [WT ($M = 9 \pm 1.2$) vs. *Gclm KO* ($M = 5.8 \pm 0.4$)] cohort relative to their WT counterparts.

3.5. Anterior cingulate cortex

Beyond the neuropathological and neuroimaging evidence linking the ACC to schizophrenia (Fornito et al., 2009), we selected this brain region for analysis based on the consistent pathological involvement of this cortical structure in our previous studies (Cabungcal et al., 2013a, 2013b; Steullet et al., 2017a, 2017b). Because previous data indicated that PV cell impairment in the ACC of *Gclm* KO mice were not present at P90 (Cabungcal et al., 2013a, 2013b), we included in our analysis fully adult mice (P180). The multivariate ANOVA test shows a significant effect for age ($F_{(9,75)} = 9.7$, $p < 0.001$) and genotype ($F_{(3,31)} = 13.4$, $p < 0.001$). We observed impairment in PV-containing neurons in the ACC that

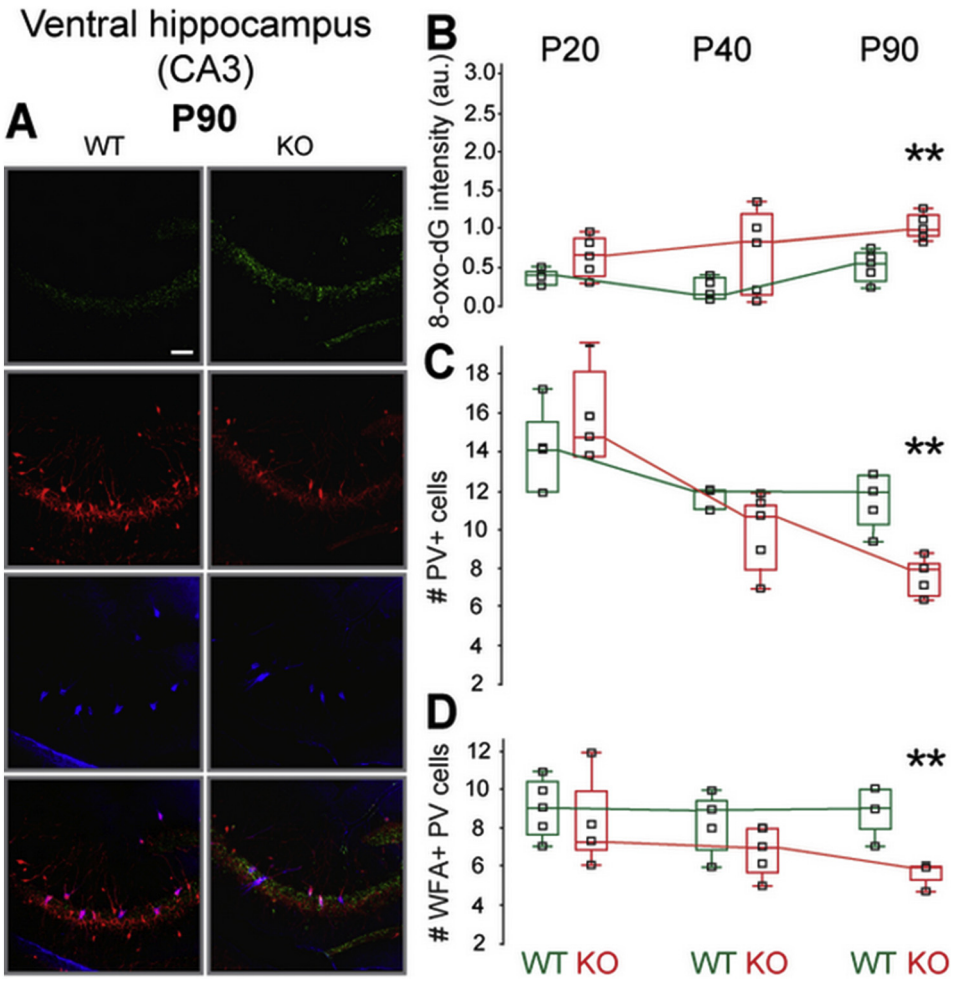

Fig. 4. Persistent redox dysregulation led to adulthood oxidative stress and adult PV+ cells deficit in the CA3 region of the ventral hippocampus of *Gclm* KO compared to WT mice. (A) Micrographs show immunofluorescent labeling for 8-oxo-dG (green), PV+ cells (red) and WFA+ PNN (blue) in the ventral hippocampus CA3 region of P90 (adult) *Gclm* KO mice. (B) 8-oxo-dG intensity (arbitrary unit, a.u.) in KO was significantly increased only when the mouse reached P90 (adulthood). (C) The number of PV+ cells, and (D) WFA+ PV cells, decreased in CA3 of KO only in P90 (adulthood). For each group, n = 5. Scale: 80 μm. Each bar depicts where the 25 and 75% of data points lie. $^{**}p = 0.01$ (pair-wise Dunnett's tests). KO, knock out; PV, parvalbumin; WFA, *Wisteria floribunda* agglutinin; WT, wild type.

emerged at P180. Immunofluorescent images of ACC from an animal at P180 are illustrated in Fig. 5A. An initial two-way multivariate ANOVA on 8-oxo-dG labeling revealed a significant overall effect of age on 8-oxo-dG expression intensity (Fig. 5B: $F_{(3,33)} = 12.9$, $p < 0.0001$) and a significant main effect of genotype (Fig. 5B: $F_{(1,33)} = 17.1$, $p = 0.0002$). An interaction effect arising from the genotype and age on 8-oxo-dG expression intensity was also observed (Fig. 5B: $F_{(3,33)} = 27.6$, $p < 0.0001$). Post-hoc comparisons revealed a significant increase in 8-oxo-dG in *Gclm* KO as compared to WT mice, from P20 to P180. Additionally, we found a significant age effect (Fig. 5C: $F_{(3,33)} = 7.9$, $p = 0.0004$) and genotype effect on PV cell density (**Fig. 5C**: $F_{(1,33)} = 4.4$, $p = 0.04$). Post-hoc comparisons identified a significant reduction in the number of PV cells stemming from the *Gclm* KO mice in the P180 [WT ($M = 65.2 \pm 7.0$) vs. *Gclm KO* ($M = 48 \pm 7.3$)] cohort relative to WT controls. In addition, an interaction effect stemming from the genotype and age on the number of PV neurons enwrapped by PNNs was observed (Fig. 5D: $F_{(3,33)} = 3.9$, $p = 0.02$). Post-hoc comparisons revealed a significant reduction in the number of PV cells surrounded by a PNN in *Gclm* KO mice in the P20 [WT ($M = 75.2 \pm 13.8$) vs. *Gclm KO* ($M = 70.8 \pm 2.2$)] and the P40 [WT ($M = 73.2 \pm 7.0$) vs. *Gclm KO* ($M = 72 \pm 8.6$)] cohort relative to WT controls. The PNN deficit observed at young age appears to reflect a delayed maturation of this extracellular matrix.

3.6. A spatio-temporal deficit in parvalbumin neurons and perineuronal nets

Our analysis revealed a distinct spatio-temporal sequence of oxidative stress induced deficit in PV-containing neurons progressing from sub-cortical to cortical brain regions in a consecutive manner, in what appeared to mimic the “domino effect” (Fig. 6). Specifically we observed an oxidative stress related impairment in PV neurons that originated from a sub-cortical source, namely the TRN, at P20 (through to P90, with no likelihood of recovery) was followed by a deficit in PV cells in the AMY at P40 (through to P90, with no likelihood of recovery). The oxidative stress induced impairment in PV cells subsequently spread to both the LGP and VH at P90 (also with no likelihood no recovery) with a cortical region, namely the ACC, being the last of the investigated brain structures to exhibit deficits in PV cells at P180.

4. Discussion

In this study, we used an animal model of oxidative stress susceptibility to address the neurodevelopmental relationship between redox dysregulation and the integrity of the PV-expressing neurons in selected cortical and sub-cortical brain regions. Our main findings include: (i) oxidative stress-induced phenotype loss

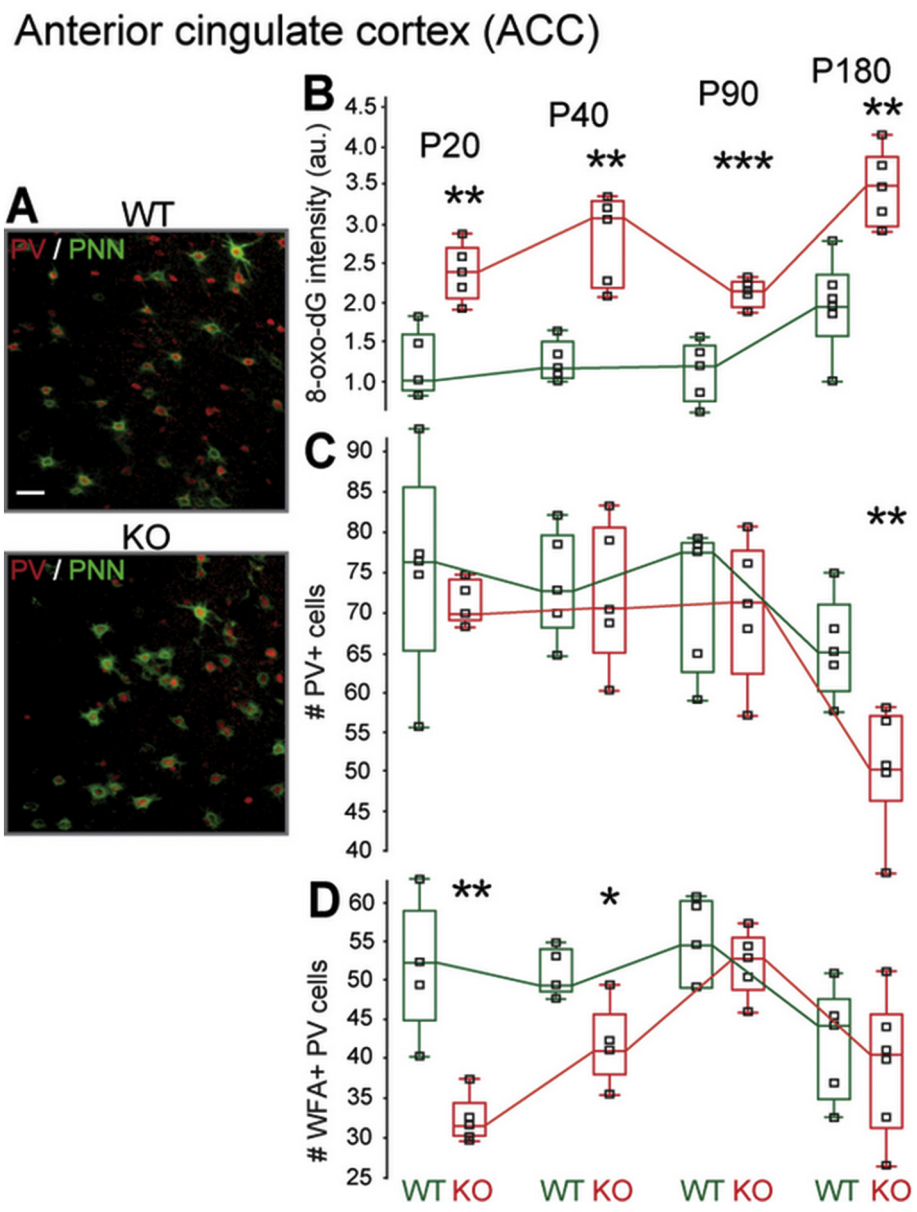

Fig. 5. Persistent redox dysregulation led to early and persisting oxidative stress affecting only adulthood PV+ cells deficit in the anterior cingulate cortex (ACC) of *Gclm* KO compared to WT mice. (A) Micrographs show immunofluorescent labeling for PV+ cells (red) and WFA (PNN) in the ACC of P180 (adult) *Gclm* WT and KO mice. (B) 8-oxo-dG intensity (arbitrary unit, a.u.) in KO (red) was significantly increased in all four age groups (P20, P40, P90 and P180). (C) The number of PV+ cells was decreased in ACC of KO only in P180 (fully adult) mice. (C) The number of PV+ cells surrounded by PNN (WFA+ PV cells) was significantly reduced in P20 and P40 KO mice, compared with WT mice, indicating a delayed formation of PNN around PV+ cells. These findings are consistent with our previous published data (Cabungcal et al., 2013b). These ACC measurements were from the same animals used to analyze TRN, AMY, LGP and CA3. For each group, n = 5. *$p = 0.05$; **$p = 0.01$, ***$p < 0.001$ (pair-wise Dunnett's tests). KO, knock out; PV, parvalbumin; WFA, *Wisteria floribunda* agglutinin; PNN, perineuronal net; WT, wild type.

of PV neurons extends beyond cortical regions (e.g. ACC and VH) to sub-cortical structures including the LGP, AMY and TRN, (ii) PV neurons located in different brain regions exhibit selective temporal sequence of vulnerability to oxidative stress during different epochs of neurodevelopment, and (iii) PV neuron impairments in sub-cortical regions precede those in cortical structures.

To our knowledge, this is the first study to describe developmental abnormalities related to oxidative stress induced PV impairment in sub-cortical regions and to report PV and PNN deficits in the LGP. The LGP is predominantly made up of PV cells that exert a strong inhibitory influence within the basal ganglia as they project to the striatum, substantia nigra reticulata/compacta and subthalamus nucleus (Saunders et al., 2016). The neuropathology of the LGP in relation to schizophrenia has not been researched in as much depth as the other sub-cortical structures evaluated herein (Bogerts et al., 1985). However, there is solid evidence for abnormal cortico-striato-pallado-thalamo-cortical circuits in schizophrenia (Avram et al., 2018). Indeed, a positive correlation between symptom severity and the volume of the external (or lateral) globus pallidus has been reported (Spinks et al., 2005). Similarly, hyperactivity of the globus pallidus was found to correlate to the severity of negative symptoms in patients with schizophrenia (Avram et al., 2018; Galeno et al., 2004; Spinks et al., 2005). Our study now shows that PV neurons within this part of the basal ganglia circuitry are vulnerable to oxidative stress.

In contrast to the LGP, a vast number of neuropathological studies exist linking the TRN and AMY to schizophrenia (i.e. Ferrarelli and Tononi, 2011; Benes, 2010). Indeed, the oxidative

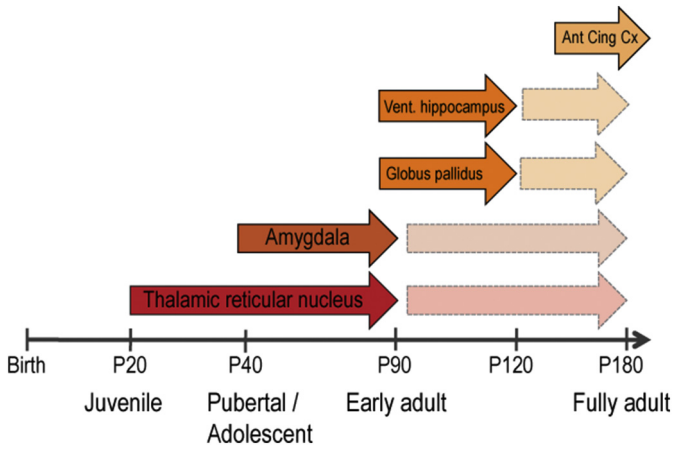

Fig. 6. Temporal sequence of PV+ cell deficit measured in different brain regions of mice with a developmental redox dysregulation (Gclm KO mice). PV+ cells were present in all these brain regions: modestly distributed in AMY, CA3 and ACC and very densely distributed in TRN and LGP. Our analysis revealed a spatio-temporal sequence of PV+ cell deficit beginning with the TRN at P20 (until P90, with likelihood of no recovery) followed by PV+ cells deficit in the Amygdala at P40 (until P90, likely with no recovery), then in the lateral globus pallidus (LGP) and CA3 of ventral hippocampus (VH) at P90 (also likely no recovery) and finally by PV+ cell deficits in the ACC at P180 (fully adult). Solid arrow shows the beginning, and maintenance, of PV+ cell deficit in *Gclm* KO mice as shown by the data in results. Dotted arrow depicts the PV+ cell deficit that is likely continuous until fully adulthood (P180) or even permanent (not analyzed).

stress induced PV deficits observed in the AMY and TRN of the mutant mice are in close alignment with the loss of PNNs and PV observed in these same regions in postmortem brains of individuals with schizophrenia (Steullet et al., 2017b; Pantazopoulos et al., 2010). At the cortical level, our observation of PV and PNN deficits in the ACC and VH replicated our previous findings (Steullet et al., 2010, 2017a; Cabungcal et al., 2013a, 2013b), confirming the susceptibility to oxidative stress of PV neurons within these cortical structures, which also display PV neuron anomalies in SZ patients (Zhang and Reynolds, 2002).

As previously mentioned, brain regions were carefully selected based upon the presence of PV expression and their clinical relevance to schizophrenia. This approach may, however, fall short in that it does not represent a "non-biased" search for oxidative stress induced PV neuron impairment. Indeed, PV cells located in other brain regions might be similarly affected by oxidative stress. Future studies applying a non-biased approach to evaluate other brain regions not investigated in this study will prove important in order to improve our neuropathological knowledge regarding the extent of oxidative stress-induced PV cell impairment that takes place in the brain, so as to better translate these observations for potential utility in clinical psychiatry.

Parvalbumin immunoreactive (PV-IR) cells are present in numerous regions of the rodent central nervous system (Celio and Heizmann, 1981; Celio, 1990; del Río et al., 1994; Alfahel-Kakunda and Silverman, 1997). However, the timing of their maturation varies across between regions. In the cortex, PV-IR cells first appear in the parietal and retrosplenial regions at postnatal day (P) 10. From P12, PV-IR cells emerge in the second parietal, cingular, frontal, hindlimb-forelimb, temporal, primary, secondary occipital and gustatory cortices, and from P15, PV-IR cells are present in the remaining regions. Generally, PV-IR cells first appear in the primary sensory/motor areas, and then in second sensory/motor or associative areas. The maturation of PV-IR cells, however, is a long-lasting process, and only completed until adult stages (del Río et al., 1994). In all cortical regions, PV-IR cells are present first in layer V, before spreading to the upper and inner cortical layers at subsequent developmental stages. PV-IR cells appear to mature much earlier in subcortical than in cortical areas. For instance, in the TRN, PV is already expressed at P0 and completed at P30 (Majak et al., 1998). In the hippocampus, PV-IR is only detected after P7 (Nitsch et al., 1990). We have found no published data detailing when PV-IR cells initially appear in the basolateral amygdala, but it is probably before P7 as it has been shown that at P16 they are functional and have acquired principal neuron connections (Woodruff and Sah, 2007). Interestingly, with the notable exception of the ACC, oxidative stress and PV neuron alterations first occur in areas (subcortical) where these neurons undergo an earlier maturation. Thus, the cumulative time of redox dysregulation may eventually impend on the structural and functional integrity of PV-IR neurons.

Excitingly, our findings also suggest that PV neurons located in different cortical and sub-cortical brain regions exhibit selective vulnerability to oxidative stress during different phases of neurodevelopment. An illustration of these spatio-temporal deficits in PV neurons can be observed in Fig. 6. This stems from inter-regional differences in 1) vulnerability to present oxidative stress and 2) susceptibility / resiliency of PV neurons toward oxidative stress. Thus in *Gclm* KO mice, TRN and ACC display signs of oxidative stress as early as P20, while oxidative stress in VH becomes only significant at P90. Interestingly, we previously reported that the dorsal hippocampus, as opposed to the VH, did not display oxidative stress and PV deficits in P90 *Gclm* KO mice (Steullet et al., 2010). Furthermore, TRN and ACC PV neurons are not equally susceptible to oxidative stress at the same time. PV neurons in the ACC appear more resistant than PV neurons in the TRN. Indeed in the ACC (if we exclude the delayed maturation at young age), apparent PV impairments are only observed at P180, while in the TRN they are already present at P20. The reasons for these differences remain unclear and require further investigation. Potential explanations include region specific differences in 1) maturation time course of PV neurons and their PNN, 2) neuronal and metabolic activity, 3) antioxidant capacity of PV neurons and their neighbored cells, 4) levels of catecholamines (dopamine, noradrenaline) that are known to generate reactive oxygen species during their auto-oxidation and catabolism.

One of the proposed mechanisms that could contribute to the sequential oxidative damage to PV neurons observed in our study stems from region specific differences in maturation time course of PV neurons. A key marker of physiologically mature PV neurons is the PNN (Hensch, 2005). This extracellular matrix is known to influence synaptic plasticity, but also protect PV neurons against oxidative stress in the ACC (Cabungcal et al., 2013a; Bitanihirwe et al., 2016). Thus, an additional oxidative insult (i.e., induced by stress) either during juvenile or adolescence can lead to PV neuron impairments in the ACC already present at P20 and P40 (Cabungcal et al., 2013a). This early susceptibility of PV neurons in the ACC is associated with the presence of an immature PNN. In contrast, PV neurons in the ACC in young adults are less affected by oxidative challenge as they are protected by a mature PNN (Cabungcal et al., 2013a, 2013b). This finding is consistent with the proposed notion that the adolescent period constitutes a critical time for the refinement of GABAergic functions in the PFC rodents and primates (Caballero and Tseng, 2016). Hence, a particular critical period would be when significant oxidative stress occurs during the time of maturation of the PV neurons while they are void of, or bear immature PNNs.

Another mechanism that may underlie the spatio-temporal deficits of PV neurons stemming from oxidative stress involves the switching of the NR2B subunit for the NR2A subunit at N-Methyl-D-Aspartate (NMDA) receptors during neurodevelopment (Monyer et al., 1994). Notably, in contrast to the NR2B unit, the NR2A subunit is preferentially expressed in PV neurons (Kinney

et al., 2006), and is highly sensitive to redox modulation (Behrens et al., 2007; Lipton et al., 2002). Therefore, redox imbalance during neurodevelopment could attenuate NMDA-R function altering the phenotype of PV-containing neurons and in the process leading to cellular injury (Hasam-Henderson et al., 2018). Activation of synaptic NMDA-Rs boosts intrinsic antioxidant defenses, through transcriptional control of the GSH, thioredoxin and peroxiredoxin systems to support antioxidant defense. NMDA-R hypo-activity during development would thus lead to the deleterious loss of this control (Baxter et al., 2015; Papadia et al., 2008). Functional deletion of NR2A confers a susceptibility to oxidative stress, microglia activation, and oxidative stress-induced PV neuron impairments in the ACC (Cardis et al., 2018). Interestingly, TRN neurons mostly express NR2B and NR2C (even at adulthood: Wenzel et al., 2000; Zhang et al., 2012) therefore lacking the NR2A-mediated signaling cascades, which boost antioxidant capacities. Thus, the defense mechanisms of PV neurons could differ from one region to another, therefore contributing to the observed differences in susceptibility across brain structures.

Temporal changes in functional connectivity between brain regions may represent yet another mechanism to explain at least some of the spatio-temporal deficits of PV neurons that we observed. Interestingly, the subcortical circuitry, including the thalamocortical circuit, appears to undergo heightened plasticity (in terms of circuitry maturation) earlier than cortical neuronal circuitry (Barkat et al., 2011). Via a domino-like mechanism, a PVI impairment in one brain region could favor PV deficit in another structure through connectivity alterations between these two regions. Thus, (1) amygdala hyper-activation stemming from $GABA_A$ receptor blockade (using picrotoxin), and (2) hyperactivity in basolateral amygdala in rat MAM model could lead to a reduction in the expression of PV in the ventral hippocampus (Berretta et al., 2004; Du and Grace, 2016). Interestingly, amygdala inputs project in CA3 but not CA1 (CA3 being the region most affected in *Gclm* KO) (Berretta et al., 2001, 2004). This could potentially explain why PV impairments in the AMY precede those in VH. Other evidence has demonstrated an increase in functional connectivity between the ventral hippocampus and the medial prefrontal cortex during neurodevelopment, with PV-containing neurons in both these structures undergoing a mutual up-regulation throughout the peri-adolescent transition to adulthood (Caballero et al., 2013, 2014). Because the ventral hippocampus sends direct projections to the medial prefrontal cortex, a PV deficit in the VH could therefore favor later PV cell impairments in the prefrontal cortex. In this context, one might tentatively speculate that some of the spatio-temporal deficits of PV neurons observed herein may arise from an increased connectivity between the sub-cortical and cortical regions, which may then lead to an increased activity of PV neurons. This could eventually become pathological (i.e., mitochondrial bioenergetic dysfunction) and disrupt PV cell intrinsic physiology and network connectivity (Inan et al., 2016; Khan, 2016), especially in conditions of compromised regulations of antioxidant systems.

A number of genetic and/or environmental animal models relevant to schizophrenia display PV neuron impairments in the mPFC and/or hippocampus at adulthood (Balu et al., 2013; Lodge et al., 2009; Meechan et al., 2015; Pitts et al., 2012; Lin et al., 2014). In the ACC, PV neuron and PNN anomalies have been associated with oxidative stress in a number of these models, suggesting convergent pathological mechanisms (Steullet et al., 2017a, 2017b). However, data on the emergence of a PV neuronal deficit during postnatal development and across different brain regions are still sparse in other animal models than *Gclm* KO mice. Thus, we cannot exclude that according to the different genetic and environmental risk factors, that some of the sequential PV-IR anomalies described in the present study might not completely overlap or correspond. In some rodent models (e.g., MAM, prenatal immune activation and human deletion/mutation model), decreased number of PV-IR neurons in the VH is observed in younger age than in the *Gclm* KO mice (Lodge et al., 2009; Giovanoli et al., 2015; Schmalbach et al., 2015). This could be associated with the severe impact of early-life stress on the hippocampus. Thus, stress may shape how PV neuron impairments emerge and develop across different brain regions. However, we postulate that many different animal models will share largely similar sequential impairments of PV neurons. Further studies investigating the impact of different genetic and environmental factors on the developmental occurrence of PV neuron deficits within the brain are therefore warranted, in order to understand the emergence of anomalies at circuit levels in patients as the disease progresses. Taking into consideration the macrostructural and neurochemical evidence, imaging studies reveal that specific brain regions within several large-scale brain circuits are already affected in high clinical high-risk subjects before the onset of full psychosis (Fusar-Poli, 2012; Dutt et al., 2015). Among the areas that display early alterations are the prefrontal and temporal cortical regions in addition to the thalamus and hippocampus (Mubarik and Tohid, 2016; Harrisberger et al., 2016). Connectivity between large-scale circuits encompassing the PFC, striatum, thalamus and cerebellum is altered during the prodromal stage and further deteriorates with the emergence of psychosis (Cao et al., 2019). Although it is not possible to directly relate the macroscopic alterations observed by imaging with the disrupted integrity of PV neurons, it is worth noting that early PV deficit in *Gclm* KO mice are found in regions belonging to these altered circuits. Environmental stressors causing a perturbation of the HPA axis during childhood and adolescence and that impact the amygdala, hippocampus and the maturation of the prefrontal cortex may eventually result in a dysregulation of the dopaminergic system leading to psychosis. Our observation remains consistent with the framework of psychosis whereby the course of the disease is initiated by a disruption of brain development (pre-morbid phase), followed by brain reorganization (prodromal phase), strongly implicated in the pathophysiology of the disease. These two aspects may lead to a phase characterized by onset of psychotic symptoms, which often fluctuate, and if left untreated leads to further deterioration of these symptoms (Millan et al., 2016).

In summary, this study reveals a spatio-temporal sequence of oxidative stress-induced PV cell impairment in sub-cortical and cortical regions of the brain. We propose that different brain regions are developmentally susceptible to oxidative stress and that anomalies in neurodevelopmental metabolic regulation stemming from oxidative stress can interfere with neural circuit maturation and functional connectivity contributing to the emergence of schizophrenia and other developmental psychopathology.

Conflict of interest

All authors declare that they have no conflict of interest.

Contributors

Dr. J-H Cabungcal, Dr. P Steullet, Dr. M Cuenod and Dr. K Do designed the study and wrote the protocol. Dr. J-H Cabungcal conducted the experiments, the analysis, and wrote the first draft of the manuscript, and Dr. R Kraftsik undertook the statistical analysis. All authors contributed to and have approved the final manuscript.

Acknowledgements

We thank Adeline Cottier for helpful technical support, Dr. Byron Bitanihirwe for assisting with the preparation of the manuscript, and Dr. Fulvio Magara of the Centre d'Etudes du

Comportement, Center for Psychiatric Neuroscience, CHUV, for support in animal facilities. We also thank our financial supports: National Center of Competence in Research (NCCR) 'SYNAPSY — The Synaptic Bases of Mental Diseases' from the Swiss National Science Foundation (no 51NF40-185897 to KQD), Damm-Etienne Foundation and Alamaya Foundation.

References

Alfahel-Kakunda A, Silverman WF (1997). Calcium-binding proteins in the substantia nigra and ventral tegmental area during development: correlation with dopaminergic compartmentalization. Brain Res Dev Brain Res. 20;103(1):9–20.

Avram, M., Brandl, F., Bäuml, J., Sorg, C., 2018. Cortico-thalamic hypo- and hyperconnectivity extend consistently to basal ganglia in schizophrenia. Neuropsychopharmacology. 43 (11), 2239–2248.

Balu, D.T., Li, Y., Puhl, M.D., Benneyworth, M.A., Basu, A.C., Takagi, S., et al., 2013. Multiple risk pathways for schizophrenia converge in serine racemase knockout mice, a mouse model of NMDA receptor hypofunction. Proc. Natl. Acad. Sci. U. S. A. 110, E2400–E2409.

Barkat, T.R., Polley, D.B., Hensch, T.K., 2011. A critical period for auditory thalamocortical connectivity. Nat. Neurosci. 14 (9), 1189–1194.

Baxter, P.S., Bell, K.F., Hasel, P., Kaindl, A.M., Fricker, M., Thomson, D., Cregan, S.P., Gillingwater, T.H., Hardingham, G.E., 2015. Synaptic NMDA receptor activity is coupled to the transcriptional control of the glutathione system. Nat. Commun. 6, 6761.

Beasley, C.L., Reynolds, G.P., 1997. Parvalbumin-immunoreactive neurons are reduced in the prefrontal cortex of schizophrenics. Schizophr. Res. 24, 349–355 (1997).

Behrens, M.M., Ali, S.S., Dao, D.N., Lucero, J., Shekhtman, G., Quick, K.L., Dugan, L.L., 2007. Ketamine-induced loss of phenotype of fast-spiking interneurons is mediated by NADPH-oxidase. Science. 318, 1645–1647.

Benes, F.M., 2010. Amygdalocortical circuitry in schizophrenia: from circuits to molecules. Neuropsychopharmacology. 35 (1), 239–257.

Benes, F.M., Berretta, S., 2001. GABAergic interneurons: implications for understanding schizophrenia and bipolar disorder. Neuropsychopharmacology. 25, 1–27.

Benes, F.M., McSparren, J., Bird, E.D., SanGiovanni, J.P., Vincent, S.L., 1991. Deficits in small interneurons in prefrontal and cingulate cortices of schizophrenic and schizoaffective patients. Arch. Gen. Psychiatry 48, 996–1001.

Benes, F.M., Lim, B., Matzilevich, D., Walsh, J.P., Subburaju, S., Minns, M., 2007. Regulation of the GABA cell phenotype in hippocampus of schizophrenics and bipolars. Proc. Natl. Acad. Sci. U. S. A. 104, 10164–10169.

Berretta, S., Munno, D.W., Benes, F.M., 2001. Amygdalar activation alters the hippocampal GABA system: "partial" modelling for postmortem changes in schizophrenia. J. Comp. Neurol. 431 (2), 129–138.

Berretta, S., Lange, N., Bhattacharyya, S., Sebro, R., Garces, J., Benes, F.M., 2004. Long-term effects of amygdala GABA receptor blockade on specific subpopulations of hippocampal interneurons. Hippocampus. 14 (7), 876–894.

Bitanihirwe, B.K., Mauney, S.A., Woo, T.U., 2016. Weaving a net of neurobiological mechanisms in schizophrenia and unraveling the underlying pathophysiology. Biol. Psychiatry 80 (8), 589–598.

Bogerts, B., Meertz, E., Schönfeldt-Bausch, R., 1985. Basal ganglia and limbic system pathology in schizophrenia. A morphometric study of brain volume and shrinkage. Arch. Gen. Psychiatry 42 (8), 784–791.

Caballero, A., Tseng, K.Y., 2016. GABAergic function as a limiting factor for prefrontal maturation during adolescence. Trends Neurosci. 39 (7), 441–448. https://doi.org/10.1016/j.tins.2016.04.010 (Epub 2016 May 24).

Caballero, A., Diah, K.C., Tseng, K.Y., 2013. Region-specific upregulation of parvalbumin-, but not calretinin-positive cells in the ventral hippocampus during adolescence. Hippocampus. 23 (12), 1331–1336.

Caballero, A., Thomases, D.R., Flores-Barrera, E., Cass, D.K., Tseng, K.Y., 2014. Emergence of GABAergic-dependent regulation of input-specific plasticity in the adult rat prefrontal cortex during adolescence. Psychopharmacology 231 (8), 1789–1796.

Cabungcal, J.H., Nicolas, D., Kraftsik, R., Cuénod, M., Do, K.Q., Hornung, J.P., 2006. Glutathione deficit during development induces anomalies in the rat anterior cingulate GABAergic neurons: relevance to schizophrenia. Neurobiol. Dis. 22 (3), 624–637.

Cabungcal, J.H., Steullet, P., Kraftsik, R., Cuenod, M., Do, K.Q., 2013. Early-life insults impair parvalbumin interneurons via oxidative stress: reversal by N-acetylcysteine. Biol. Psychiatry 73 (6), 574–582.

Cabungcal, J.H., Steullet, P., Morishita, H., Kraftsik, R., Cuenod, M., Hensch, T.K., Do, K.Q., 2013. Perineuronal nets protect fast-spiking interneurons against oxidative stress. Proc. Natl. Acad. Sci. U. S. A. 110 (22), 9130–9135.

Cao H, Chung Y, McEwen SC, Bearden CE, Addington J, Goodyear B, Cadenhead KS, Mirzakhanian H, Cornblatt BA, Carrión R, Mathalon DH, McGlashan TH, Perkins DO, Belger A, Seidman LJ, Thermenos H, Tsuang MT, van Erp TGM, Walker EF, Hamann S, Anticevic A, Woods SW, Cannon TD (2019). Progressive reconfiguration of resting-state brain networks as psychosis develops: preliminary results from the North American Prodrome Longitudinal Study (NAPLS) consortium. Schizophr Res, 28. pii: S0920-9964(19)30024-6. doi:https://doi.org/10.1016/j.schres.2019.01.017.

Cardis, R., Cabungcal, J.H., Dwir, D., Do, K.Q., Steullet, P., 2018. A lack of GluN2A-containing NMDA receptors confers a vulnerability to redox dysregulation: consequences on parvalbumin interneurons, and their perineuronal nets. Neurobiol Dis. 109 (Pt A), 64–75.

Celio, M.R., 1990. Calbindin D-28k and parvalbumin in the rat nervous system. Neuroscience. 35 (2), 375–475 (1990).

Celio MR, Heizmann CW (1981). Calcium-binding protein parvalbumin as a neuronal marker. Nature., 24;293(5830):300–2.

Crick, F., 1984. Function of the thalamic reticular complex: the searchlight hypothesis. Proc. Natl. Acad. Sci. U. S. A. 81 (14), 4586–4590.

del Río, J.A., de Lecea, L., Ferrer, I., Soriano, E., 1994. The development of parvalbumin-immunoreactivity in the neocortex of the mouse. Brain Res. Dev. Brain Res. 81 (2), 247–259.

Do, K.Q., Cabungcal, J.H., Frank, A., Steullet, P., Cuenod, M., 2009. Redox dysregulation, neurodevelopment, and schizophrenia. Curr. Opin. Neurobiol. 19 (2), 220–230.

Du Y, Grace AA (2016). Amygdala hyperactivity in MAM model of schizophrenia is normalized by peripubertal diazepam administration. Neuropsychophar., 41(10): 2455–62. doi:10.101038/npp.2016.42.

Dutt, A., Tseng, H.H., Fonville, L., Drakesmith, M., Su, L., Evans, J., Zammit, S., Jones, D., Lewis, G., David, A.S., 2015. Exploring neural dysfunction in 'clinical high risk' for psychosis : a quantitative review of fMRI. J. Psychiatr. Res. 61, 122–134.

Dwir, D., Cabungcal, J.H., Tenenbaum, L., Steullet, P., Cuenod, M., Do, K.Q., 2017. Matrix metalloproteinase inhibition prevents the adult excitatory-inhibitory imbalance induced by the reciprocal interaction between neuroinflammation and oxidative stress during development. Schizophr. Bull. 43 (Suppl. 1), S32.

Ferrarelli, F., Tononi, G., 2011. The thalamic reticular nucleus and schizophrenia. Schizophr. Bull. 37 (2), 306–315.

Fornito, A., Yücel, M., Pantelis, C., 2009. Reconciling neuroimaging and neuropathological findings in schizophrenia and bipolar disorder. Curr. Opin. Psychiatry 22 (3), 312-9. https://doi.org/10.1097/YCO.0b013e32832a1353. Review.

Fusar-Poli, F., 2012. Voxel-wise meta analysis of fMRI studies in patients at clinical high risk for psychosis. J. Psychiatry Neurosci. 37 (2), 106–112.

Galeno, R., Molina, M., Guirao, M., Isoardi, R., 2004. Severity of negative symptoms in schizophrenia correlated to hyperactivity of the left globus pallidus and the right claustrum. A PET study. World J Biol Psychiatry. 5 (1), 20–25.

Giovanoli, S., Notter, T., Richetto, J., Labouesse, M.A., Vuillermot, S., Riva, M.A., Meyer, U., 2015. Late prenatal immune activation causes hippocampal deficits in the absence of persistent inflammation across aging. Neuroinflammation, 25, 12, 221. https://doi.org/10.1186/s12974-015-0437-y.

Gonzalez-Burgos, G., Cho, R.Y., Lewis, D.A., 2015. Alterations in cortical network oscillations and parvalbumin neurons in schizophrenia. Biol. Psychiatry 77 (12), 1031–1040.

Graybiel, A.M., 1997. The basal ganglia and cognitive pattern generators. Schizophr. Bull. 23 (3), 459–469.

Halassa, M.M., Acsády, L., 2016. Thalamic inhibition: diverse sources, diverse scales. Trends Neurosci. 39 (10), 680–693.

Harrisberger, F., Buechler, R., Smieskova, R., Lenz, C., Walter, A., Egloff, L., Bendfeldt, K., Simon, A.E., Wortuba, D., Theodoridou, A., Rossler, W., Riecher-Rossler, A., Land, U.E., Heekeren, K., Borgwardt, S., 2016. Alterations in the hippocampus and thalamus in individuals at high risk psychosis. NPJ Schizophr. 28 (2), 16033.

Hasam-Henderson, L.A., Gotti, G.C., Mishto, M., Klisch, C., Gerevich, Z., Geiger, J.R.P., Kovács, R., 2018. NMDA-receptor inhibition and oxidative stress during hippocampal maturation differentially alter parvalbumin expression and gamma-band activity. Sci. Rep. 22 (8(1)), 9545.

Hashimoto, T., Volk, D.W., Eggan, S.M., Mirnics, K., Pierri, J.N., Sun, Z., Sampson, A.R., Lewis, D.A., 2003. Gene expression deficits in a subclass of GABA neurons in the prefrontal cortex of subjects with schizophrenia. J. Neurosci. 23, 6315–6326.

Hensch, T.K., 2005. Critical period plasticity in local cortical circuits. Nat. Rev. Neurosci. 6 (11), 877–888.

Inan, M., Zhao, M., Manuszak, M., Karakaya, C., Rajadhyaksha, A.M., Pickel, V.M., Schwartz, T.H., Goldstein, P.A., Manfredi, G., 2016. Energy deficit in parvalbumin neurons leads to circuit dysfunction, impaired sensory gating and social disability. Neurobiol. Dis. 93, 35–46.

Jones, E.G., Hendry, S.H., 1989. Differential calcium binding protein immunoreactivity distinguishes classes of relay neurons in monkey thalamic nuclei. Eur. J. Neurosci. 1 (3), 222–246.

Kann, O., 2016. The interneuron energy hypothesis: implications for brain disease. Neurobiol. Dis. 90, 75–85.

Kann O, Huchzermeyer C, Kovács R, Wirtz S, Schuelke M. (2011) Gamma oscillations in the hippocampus require high complex I gene expression and strong functional performance of mitochondria. Brain. 134(Pt 2):345–58.

Kann, O., Papageorgiou, I.E., Draguhn, A., 2014. Highly energized inhibitory interneurons are a central element for information processing in cortical networks. J. Cereb. Blood Flow Metab. 34 (8), 1270–1282.

Kinney, J.W., Davis, C.N., Tabarean, I., Conti, B., Bartfai, T., Behrens, M.M., 2006. A specific role for NR2A-containing NMDA receptors in the maintenance of parvalbumin and GAD67 immunoreactivity in cultured interneurons. J. Neurosci. 26, 1604–1615.

Kulak, A., Steullet, P., Cabungcal, J-H., Werge, T., Ingason, A., Cuenod, M., Do, K.Q., 2013. Redox dysregulation in the pathophysiology of schizophrenia and bipolar disorder: insights from animal models, 20 Antioxid. Redox Signal. 18 (12), 1428-43. https://doi.org/10.1089/ars.2012.4858.

Lewis, D.A., Curley, A.A., Glausier, J.R., Volk, D.W., 2012. Cortical parvalbumin interneurons and cognitive dysfunction in schizophrenia. Trends Neurosci. 35 (1),

57–67.
Lin, H., Hsu, F.C., Baumann, B.H., Coulter, D.A., Anderson, S.A., Lynch, D.R., 2014. Cortical parvalbumin GABAergic deficits with alpha7 nicotinic acetylcholine receptor deletion: implications for schizophrenia. Mol. Cell. Neurosci. 61, 163–175.
Lipton, S.A., Choi, Y.B., Takahashi, H., Zhang, D., Li, W., Godzik, A., Bankston, L.A., 2002. Cysteine regulation of protein function–as exemplified by NMDA-receptor modulation. Trends Neurosci. 25 (9), 474–480.
Lodge, D.J., Behrens, M.M., Grace, A.A., 2009. A loss of parvalbumin-containing interneurons is associated with diminished oscillatory activity in an animal model of schizophrenia. J. Neurosci. 29, 2344–2354.
Majak, K., Berdel, B., Kowiański, P., Dziewiatkowski, J., Lipowska, M., Moryś, J., 1998. Parvalbumin immunoreactivity changes in the thalamic reticular nucleus during the maturation of the rat's brain. Folia Neuropathol. 36 (1), 7–14.
Meechan, D.W., Maynard, T.M., Tucker, E.S., Fernandez, A., Karpinski, B.A., Rothblat, L.A., et al., 2015. Modeling a model: mouse genetics, 22q11.2 deletion syndrome, and disorders of cortical circuit development. Prog. Neurobiol. 130, 1–28.
Millan, M.J., Andrieux, A., Bartzokis, G., Cadenhead, K., Dazzan, P., Fusar-Poli, P., Gallinat, J., Giedd, J., Grayson, D.R., Heinrichs, M., Kahn, R., Krebs, M.O., Leboyer, M., Lewis, D., Marin, O., Marin, P., Meyer-Lindenberg, A., McGorry, P., McGuire, P., Owen, M.J., Patterson, P., Sawa, A., Spedding, M., Uhlhaas, P., Vaccarino, F., Wahlestedt, C., Weinberger, D., 2016. Altering the course of schizophrenia: progress and perspectives. Nat. Rev. Drug Discov. 15 (7), 485–515. https://doi.org/10.1038/nrd.2016.28.
Monin, A., Baumann, P.S., Griffa, A., Xin, L., Mekle, R., Fournier, M., Butticaz, C., Klaey, M., Cabungcal, J.H., Steullet, P., Ferrari, C., Cuenod, M., Gruetter, R., Thiran, J.P., Hagmann, P., Conus, P., Do, K.Q., 2015. Glutathione deficit impairs myelin maturation: relevance for white matter integrity in schizophrenia patients. Mol. Psychiatry 20 (7), 827–838.
Monyer, H., Burnashev, N., Laurie, D.J., Sakmann, B., Seeburg, P.H., 1994. Developmental and regional expression in the rat brain and functional properties of four NMDA receptors. Neuron. 12, 529–540.
Mubarik, A., Tohid, H., 2016. Frontal lobe alterations in schizophrenia. Trends Psychiatr and Psycho 38, 4. https://doi.org/10.1590/2237-6089-2015-0088.
Nitsch, R., Bergmann, I., Küppers, K., Mueller, G., Frotscher, M., 1990. Late appearance of parvalbumin-reactivity in the development of GABAergic neurons in the rat hippocampus. Neurosci. Lett. 118 (2), 147–150.
Ohshima, T., Endo, T., Onaya, T., 1991. Distribution of parvalbumin immunoreactivity in the human brain. J. Neurol. 238 (6), 320–322.
Pantazopoulos, H., Woo, T.U., Lim, M.P., Lange, N., Berretta, S., 2010. Extracellular matrix-glial abnormalities in the amygdala and entorhinal cortex of subjects diagnosed with schizophrenia. Arch. Gen. Psychiatry 67 (2), 155–166.
Papadia, S., Soriano, F.X., Léveillé, F., Martel, M.A., Dakin, K.A., Hansen, H.H., Kaindl, A., Sifringer, M., Fowler, J., Stefovska, V., McKenzie, G., Craigon, M., Corriveau, R., Ghazal, P., Horsburgh, K., Yankner, B.A., Wyllie, D.J., Ikonomidou, C., Hardingham, G.E., 2008. Synaptic NMDA receptor activity boosts intrinsic antioxidant defenses. Nat. Neurosci. 11 (4), 476–487.
Pitts, M.W., Raman, A.V., Hashimoto, A.C., Todorovic, C., Nichols, R.A., Berry, M.J., 2012. Deletion of selenoprotein P results in impaired function of parvalbumin interneurons and alterations in fear learning and sensorimotor gating. Neuroscience 208, 58–68.
Robbins, T.W., 1990. The case of frontostriatal dysfunction in schizophrenia. Schizophr. Bull. 6 (3), 391–402.
Saunders, A., Huang, K.W., Sabatini, B.L., 2016. Globus pallidus externus neurons expressing parvalbumin interconnect the subthalamic nucleus and striatal interneurons. PLoS One 11 (2), e0149798.
Schmalbach, B., Lepsveridze, E., Djogo, N., Papashvili, G., Kuang, F., Leshchyns'ka, I., Sytnyk, V., Nikonenko, A.G., Dityatev, A., Jakovcevski, I., Schachner, M., 2015. Age-dependent loss of parvalbumin-expressing hippocampal interneurons in mice deficient in CHL1, a mental retardation and schizophrenia susceptibility gene. J. Neurochem. 135 (4), 830–844. https://doi.org/10.1111/jnc.13284 (Epub 2015 Sep 8).
Sohal, V.S., Zhang, F., Yizhar, O., Deisseroth, K., 2009. Parvalbumin neurons and gamma rhythms enhance cortical circuit performance. Nature. 459 (7247), 698–702.
Spinks, R., Nopoulos, P., Ward, J., Fuller, R., Magnotta, V.A., Andreasen, N.C., 2005. Globus pallidus volume is related to symptom severity in neuroleptic naive patients with schizophrenia. Schizophr. Res. 3 (2–3), 229–233.
Steullet, P., Cabungcal, J.H., Kulak, A., Kraftsik, R., Chen, Y., Dalton, T.P., Cuenod, M., Do, K.Q., 2010. Redox dysregulation affects the ventral but not dorsal hippocampus: impairment of parvalbumin neurons, gamma oscillations, and related behaviors. J. Neurosci. 30 (7), 2547–2558.
Steullet, P., Cabungcal, J.H., Monin, A., Dwir, D., O'Donnell, P., Cuenod, M., Do, K.Q., 2016. Redox dysregulation, neuroinflammation, and NMDA receptor hypofunction: a “central hub” in schizophrenia pathophysiology? Schizophr. Res. 176 (1), 41–51.
Steullet, P., Cabungcal, J.H., Coyle, J., Didriksen, M., Gill, K., Grace, A.A., Hensch, T.K., LaMantia, A.S., Lindemann, L., Maynard, T.M., Meyer, U., Morishita, H., O'Donnell, P., Puhl, M., Cuenod, M., Do, K.Q., 2017. Oxidative stress-driven parvalbumin interneuron impairment as a common mechanism in models of schizophrenia. Mol. Psychiatry 22 (7), 936–943.
Steullet, P., Cabungcal, J.H., Bukhari, S.A., Ardelt, M.I., Pantazopoulos, H., Hamati, F., Salt, T.E., Cuenod, M., Do, K.Q., Berretta, S., 2017. The thalamic reticular nucleus in schizophrenia and bipolar disorder: role of parvalbumin-expressing neuron networks and oxidative stress. Mol. Psychiatry 23 (10), 2057–2065. https://doi.org/10.1038/mp.2017.230 (Epub ahead of print).
Uhlhaas, P.J., Singer, W., 2015. Oscillations and neuronal dynamics in schizophrenia: the search for basic symptoms and translational opportunities. Biol. Psychiatry 77 (12), 1001–1009.
Wenzel, A., Fritschy, J.M., Mohler, H., Benke, D., 2000. N-methyl-D-aspartate receptor subunit NR2B is widely expressed throughout the rat diencephalon: an immunohistochemical study. J. Comp. Neurol. 428 (3), 428–449.
Woodruff, A.R., Sah, P., 2007. Networks of parvalbumin-positive interneurons in the basolateral amygdala. J. Neurosci. 27 (3), 553–563.
Young, A., Wimmer, R.D., 2017. Implications for the thalamic reticular nucleus in the attention and sleep in schizophrenia. Schizophr. Res. 180, 44–47.
Zhang, Z.J., Reynolds, G.P., 2002. A selective decrease in the relative density of parvalbumin-immunoreactive neurons in the hippocampus in schizophrenia. Schizophr. Res. 55, 1–10.
Zhang, Y., Buonanno, A., Vertes, R.P., Hoover, W.B., Lisman, J.E., 2012. NR2C in the thalamic reticular nucleus; effects of the NR2C knockout. PLoS One 7 (7), e41908. https://doi.org/10.1371/journal.pone.0041908.